Viscoelastic Melt Behavior of Poly(2,6-dimethyl-1,4-phenylene Oxide), High-Impact Polystyrene, and A 35–65 Blend

LAWRENCE R. SCHMIDT, *General Electric Company, Corporate Research and Development, Schenectady, New York 12301*

Synopsis

The viscoelastic melt behavior of poly(2,6-dimethyl-1,4-phenylene oxide) (PPO* resin), high-impact polystyrene (HIPS), and a 35–65 blend of these polymers has been characterized by measuring the steady shear viscosity and primary normal stress difference and the dynamic storage and loss moduli as functions of shear rate or frequency and temperature. Time–temperature superpositioning was used to generate master curves of each type of data for a reference temperature of 260°C. This procedure required five different empirical shift factors for each material. These shift factors show large differences between PPO resin and HIPS and exhibited large deviations from the WLF equation with universal constants. This result suggests that the temperature dependence of the relaxation processes in PPO resin is significantly different from the temperature dependence of HIPS relaxations. Flow activation energies computed from the viscosity data for PPO resin are much higher and more shear sensitive than those calculated for HIPS. The computed relaxation spectra clearly display the effect of long-time relaxation mechanisms associated with PPO molecules when compared to HIPS. The 35–65 blend exhibits general rheological compatibility with material parameters and responses intermediate between PPO resin and HIPS. This result is indicative of a high degree of segmental mixing for the two components in the blend.

INTRODUCTION

Physical mixing of two or more polymers is a technique which is frequently used to enhance the properties of an existing commercial polymer. Generally, polymers which are arbitrarily chosen for physical blending are incompatible, resulting in multiphase materials with poor or undesirable properties.

Single-phase blends prepared from compatible polymers are limited by the small number of known compatible polymers. Manson and Sperling[1] list seven polymer pairs that are compatible or nearly compatible. One of these pairs, poly(2,6-dimethyl-1,4-phenylene oxide) (PPO resin) and polystyrene (PS), is of particular interest because the physical properties of the homopolymers are widely different, yet blends of these polymers exhibit thermodynamic compatibility over the entire composition range.[2] A single glass transition temperature (T_g) is observed for a blend of these polymers when measured by differential scanning calorimetry or thermal optical analysis.

Since blends of PPO resin and PS or PPO and high-impact polystyrene (HIPS) are most often prepared by physical mixing with the resins in the melt phase, the particular choice of molecular weight (MW) and molecular weight distribution (MWD) of each polymer is an important consideration since these molecular parameters strongly influence the overall rheology. Of particular concern is the ability to disperse one resin in the matrix of the other since the property profile of the blend will be dependent on the level of mixing.

* PPO is a registered trademark of the General Electric Company.

Journal of Applied Polymer Science, Vol. 23, 2463–2479 (1979)

0021-8995/79/0023-2463$01.00

Prest and Porter[3] rheologically characterized blends of PPO resin and anionically polymerized atactic PS. Their measurements were restricted to temperatures below 250°C and compositions with less than 50 wt-% PPO resin. Their dynamic melt data indicate that the entanglement MW (M_e) of the blends decreases with increasing PPO content (pure PPO resin was not tested). From the computed relaxation spectra of the different blends they show that PPO molecules contribute a broad distribution of long relaxation mechanisms.

Relaxation processes in the melt are of considerable interest because they are directly related to molecular structure and strongly influence processing behavior, including mixing. This paper presents extensive rheological data on pure PPO, pure HIPS resin, and a 35–65 (% by weight) blend of these two polymers. Both viscous and elastic properties were measured to determine how the blend derives its rheological properties from the pure components and to isolate specific contributions of each polymer to the relaxation spectrum of the blend.

EXPERIMENTAL

Materials and Sample Preparation

PPO resin was obtained as a powder from G. F. Lee, Jr., General Electric Company, Plastics Division, Selkirk, New York, who also provided a sample of HIPS (Foster Grant 834, which contains about 10 wt-% polybutadiene) in the form of pellets and a 35–65 blend of these resins (35 wt-% PPO resin), also in the form of pellets. The blend was prepared in a Werner & Pfleiderer twin-screw extruder (28 mm). The PPO powder, HIPS pellets, plus a small amount of stabilizers were metered to the extruder at a constant feed rate. The extruder barrel was set at about 288°C, while the die temperature was set at 290°C. The screw speed was 260 rpm requiring 400 in.-lb torque. The extrudate was water cooled and pelletized. Molecular weight data on these as-received materials were obtained by GPC, and intrinsic viscosities (IV) were measured in chloroform at 25°C. These data are summarized in Table I. For these measurements both HIPS and the 35–65 blend were first filtered through a glass mat with 0.2–10-μm pore sizes to remove gel particles. It is quite possible that some polystyrene molecules remained with the gel particles during filtering, so the values reported in Table I for HIPS and the 35–65 blend are probably not exact.

The three different materials were compression molded into sheets measuring 10.2 cm × 10.2 cm × 0.2 cm. The plattens on the press were set at 293°C for PPO resin, at 193°C for HIPS, and at 293°C for the 35–65 blend. All samples were pressed between Teflon-coated aluminum sheets and allowed to air cool after pressing. Each sheet was cut into 25-mm and 50-mm squares for testing. Table

TABLE I
Molecular Weight Data

	As received			After compression molding		
	IV, dl/g	$\overline{M}_w$	$\overline{M}_w/\overline{M}_n$	IV, dl/g	$\overline{M}_w$	$\overline{M}_w/\overline{M}_n$
PPO Resin	0.54	50,000	4.2	0.59	70,000	4.0
HIPS	0.78	200,000	7.5	0.78	193,000	8.1
35–65 Blend	0.67	147,000	3.4	0.67	160,000	10.1

I lists intrinsic viscosities and molecular weight data for each of the molded sheet specimens.

Preliminary tests with PPO sheets were unsuccessful because trapped air and/or residual solvent from the polymerization caused considerable gassing when the specimen was loaded between the hot rheometer fixtures even though the compression-molded sheets were clear and free of bubbles. This bubble problem was eliminated by vacuum drying the test samples for at least 12 hr at 60°C and 10 mm Hg. GPC results and intrinsic viscosities on these conditioned samples indicated that there were no molecular weight changes associated with this treatment.

Bubble formation was not a problem with either HIPS or the 35–65 blend. Thus, these materials were not preconditioned before testing.

PROCEDURE

The viscoelastic properties of the different melts were measured with a Rheometrics Mechanical Spectrometer Model RMS-7200. The plate-and-cone fixtures shown schematically in Figure 1(a) were used to obtain steady shear viscosity and steady primary normal stress difference as functions of temperature and shear rate. Both 25-mm- and 50-mm-diameter fixtures (stainless steel) were used with a cone angle of 0.04 radian. The cone had been truncated to avoid accidental damage to the plate when a test specimen was loaded between the fixtures. Thus, there is a distance or gap which must be set between the small flat region on the cone and the plate. The gap, as shown in Figure 1(a), was 50 μm for each set of plate-and-cone fixtures. The gap setting is critical because it establishes spherical symmetry with the fixtures which in turn assures a simple shear flow field. The shear stress τ_{12} can be derived from the equation of motion and is related to the measured torque by the following expression:

$$\tau_{12} = 3M/2\pi R^3 \tag{1}$$

where M is the torque and R is the fixture radius. The shear rate $\dot{\gamma}$ is computed as

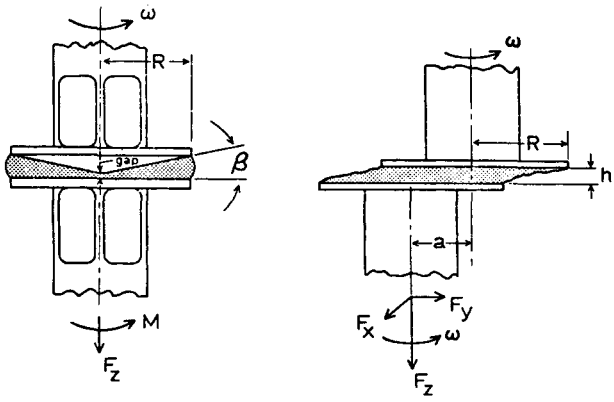

Fig. 1. Schematic of rotational rheometer test fixtures: (A) concentric plate-and-cone geometry; (B) eccentric parallel-disc geometry.

$$\dot{\gamma} = \omega/\beta \tag{2}$$

where ω is the angular speed or frequency (rad/sec) and β is the cone angle (rad). The simple shear viscosity is then, by definition,

$$\eta = \tau_{12}/\dot{\gamma} \tag{3}$$

The primary normal stress coefficient ψ_1 was computed from the measured normal force F_z from the following expression:

$$\psi_1 = \frac{N_1}{\dot{\gamma}^2} = \frac{P_{11} - P_{22}}{\dot{\gamma}^2} = \frac{2F_z}{\pi R^2 \dot{\gamma}^2} \tag{4}$$

where N_1 or $P_{11} - P_{22}$ is the primary normal stress difference.

Dynamic melt tests were run with eccentric rotating discs (ERD), Fig. 1(b). This test mode is frequently referred to as the Maxwell orthogonal rheometer. Recent studies have shown both experimentally and theoretically that ERD produce material deformations equivalent to the oscillating plate-and-cone test (see Walters,[4] for example). The shear strain γ for ERD is computed from the following expression:

$$\gamma = a/h \tag{5}$$

where a is the eccentricity and h is the spacing between the parallel discs. The storage modulus G' is computed as

$$G' = F_y h/\pi R^2 a \tag{6}$$

where F_y is the force generated collinearly with the eccentricity. The loss modulus G'' is computed as

$$G'' = F_x h/\pi R^2 a \tag{7}$$

where F_x is the force in the shear plane, orthogonal to the eccentricity.

The main advantage of the ERD test mode is that the results are much less sensitive to fixture alignment as compared to the plate-and-cone test mode, and there is no critical gap to be set. Consequently, residual stresses associated with specimen loading are seldom a serious problem.

In the above tests, specimens were loaded between the hot fixtures and sufficient time was allowed for the system to return to the desired set temperature. The separation between the fixtures was then set and excess material was cut away, leaving a neat interface. This entire operation could generally be performed in less than 5 min. However, at the lower end of the temperature range where the material behavior is somewhat leather-like, the preparation time was considerably longer.

All tests were run in a hot nitrogen atmosphere which was controlled by an environmental chamber surrounding the test fixtures. Upon completion of a test, the samples were removed from between the cooled fixtures and examined. Samples of HIPS and the blend were bubble free. Bubble formation in PPO melts, associated with thermal degradation, was monitored by reflecting a small light beam between the test fixtures which illuminated the bubbles. When bubbles were detected, the test was terminated. Prolonged testing of selected PPO samples produced only a few small bubbles, except at the melt–gas interface. However, at 300°C, thermal degradation, i.e., bubble formation, is sufficiently rapid so that several different specimens were required to cover the desired frequency range.

RESULTS AND DISCUSSION

Since the mechanical spectrometer has a somewhat limited range of test speeds or frequencies and samples seldom behave properly over the entire range of deformation rates, e.g., the melt–gas interface distorts due to an elastic instability or centrifugal forces, material responses were measured over a limited range of shear rate or frequency at several different temperatures. These data were then reduced to material parameters and shifted onto master curves to produce a very broad characterization covering many decades of deformation rate. The time–temperature superposition principle employed here assumes that all relaxation processes for each material have the same temperature dependence.

Figures 2 through 4 show loss moduli as a function of frequency and temperature for the three materials. The strain was set at 5%, which was verified to be well within the linear region of material response for these polymers. With HIPS and the blend, each test specimen was run at two consecutive temperatures. Thus, only three specimens of each material were used to generate the data in Figures 3 and 4. For PPO resin, one specimen was tested at 240° and 260°C and another at 280°C. At 300°C, three different specimens (one per decade of frequency) were required to cover the frequency range because bubble formation occurred within a short period of time after the specimen was loaded between the fixtures. The measured forces and torque at a frequency did not change until bubbles were observed. GPC results confirmed that molecular weight had not changed significantly up to the point of gassing. In addition, several internal checks, i.e., repeated measurements at one or two frequencies, were made during each run to make certain that samples were not changing in some rheologically significant manner.

A reference temperature of 260°C was arbitrarily chosen, and all of the modulus data for each sample were shifted horizontally to lie on one master curve.

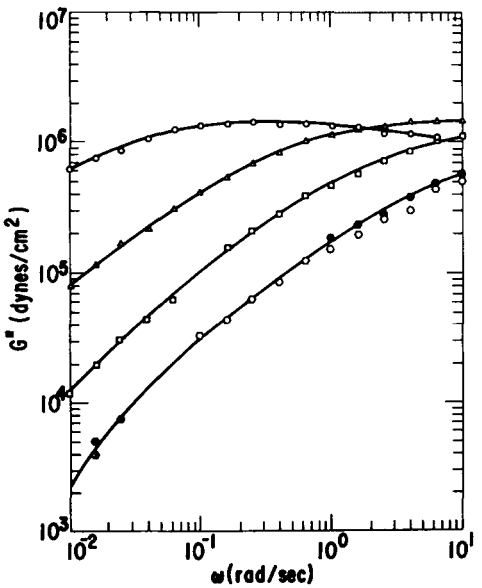

Fig. 2. Loss modulus vs frequency for poly(2,6-dimethyl-1,4-phenylene oxide): (○) 240°C; (△) 260°C; (□) 280°C; (○) 300°C.

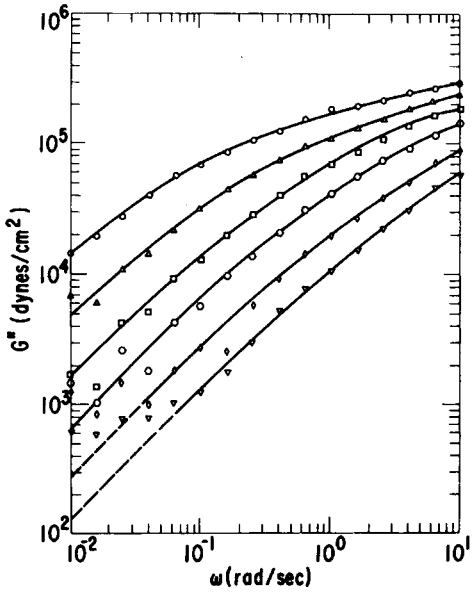

Fig. 3. Loss modulus vs frequency for high-impact polystyrene: (○) 180°C; (△) 200°C; (□) 220°C; (○) 240°C; (◇) 260°C; (▽) 280°C.

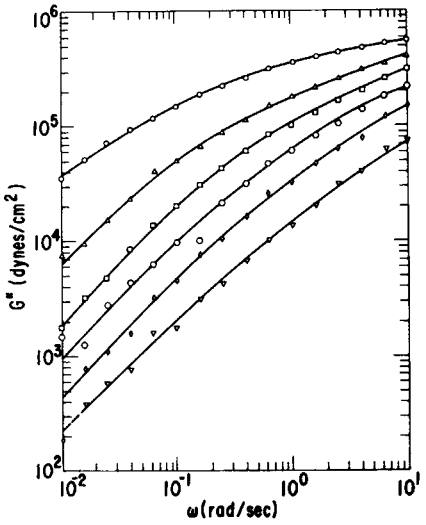

Fig. 4. Loss modulus vs frequency for a 35–36 blend: (○) 193°C; (△) 220°C; (□) 240°C; (○) 260°C; (◇) 280°C; (▽) 300°C.

The smoothed master curve of loss modulus is shown in Figure 5 for each material. The characterization now extends over 5½ decades of frequency and shows large differences between the various materials. Figure 6 shows similar master curves for the storage modulus data. As expected for compatible polymers, the response of the blend is intermediate and closer to the response of HIPS, the major component. This provides further evidence that PPO molecules are well mixed with HIPS molecules, i.e., polystyrene molecules.

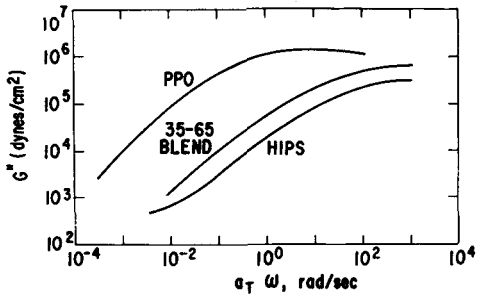

Fig. 5. Master curves of loss moduli reduced to 260°C for poly(2,6-dimethyl-1,4-phenylene oxide), high-impact polystyrene, and a 35–65 blend.

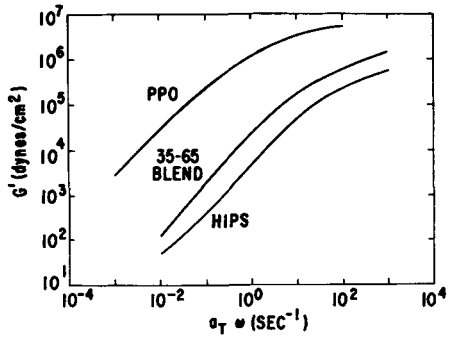

Fig. 6. Master curves of storage moduli reduced to 260°C for poly(2,6-dimethyl-1,4-phenylene oxide), high-impact polystyrene, and a 35–65 blend.

The fact that all the moduli data can be superpositioned by empirically shifting the time scale by a temperature function a_T implies that all relaxation times associated with flow mechanisms in the melt change with temperature by the same factor. This aspect will be discussed in greater detail when other experimental shift factors are presented.

The high loss modulus values at low frequencies for PPO resin reflect the very long relaxation times of this polymer. The stiffness of the polymer backbone, extent of entanglement, MW, and MWD all contribute to this response. The rubbery plateau for PPO resin occurs at a much lower frequency than the HIPS plateau and the PPO resin plateau modulus (1.5×10^6 dynes/cm^2) is about a decade higher than that displayed by HIPS (4.0×10^5 dynes/cm^2).

The G'' plateau modulus has been related to M_e by Marvin[5] who derived the following expression:

$$M_e = 0.32\rho RT/G'' \tag{8}$$

where ρ is the melt density, R is the universal gas content, and T is absolute temperature. Equation (8) is based on ideal rubber elasticity theory which treats a crosslinked rubber or in this case a physically entangled network, as if the distribution of chain segments between entanglement junctions followed a Gaussian distribution. Table II summarizes the computed entanglement molecular weights for the three different materials. The melt density for each material was assumed equal to 1 g/cm^3, which should create an error of less than

TABLE II
Entanglement Molecular Weight

Material	$G''_{plateau}$, dynes/cm^2	M_e
PPO Resin	1.5×10^6	9,100
HIPS	4.0×10^5	30,100
35–65 Blend	6.0×10^5	20,700

10%. Prest and Porter,[3] having not characterized pure PPO resin, estimated M_e(PPO resin) by extrapolating the relative modulus data at low concentrations to high concentrations, i.e., pure PPO resin. Their empirical relation, M_e(PPO resin) $\simeq M_e$(PS)/4.2, yields a M_e(PPO resin) of 4300. These values are almost half the values listed in Table II. It is not clear in their paper how they arrived at M_e(PS) = 18,000, especially since the plateau value in the G'' curve for pure PS (their Fig. 1) is about 4×10^5. This is equal to the experimentally determined value for HIPS in this study. Using this value in the empirical expression of Prest and Porter yields a M_e(PPO resin) of about 7100, substantially lower than the experimental value listed in Table II.

The viscosity and normal force data for the three materials are shown in Figures 7 through 9. A different sample was used at each temperature because the plate-and-cone fixutres were used and the gap setting is critical for meaningful results. Since loading a sheet sample into the plate-and-cone fixtures is usually a lengthy procedure, due to the time required for the loading stress to relax out, only limited data could be obtained with PPO resin. The gap could not be set at 240°C because PPO resin is much more elastic than viscous at this temperature. At 260°C the gap could be set, but the procedure lasted 1½ hr. Only three data points were obtained before the sample started to evolve gas. At 280°C

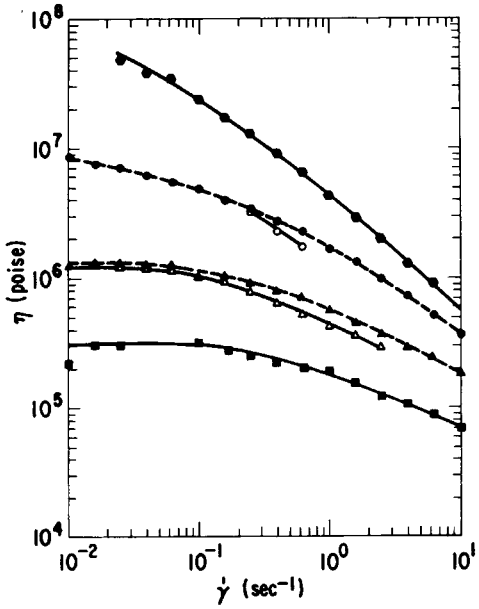

Fig. 7. Shear viscosity as function of shear rate for poly(2,6-dimethyl-1,4-phenylene oxide): (●) $|\eta^*|$ 240°C; (○) η, (●) $|\eta^*|$ 260°C; (△) η, (▲) $|\eta^*|$ 280°C; (■) $|\eta^*|$ 300°C.

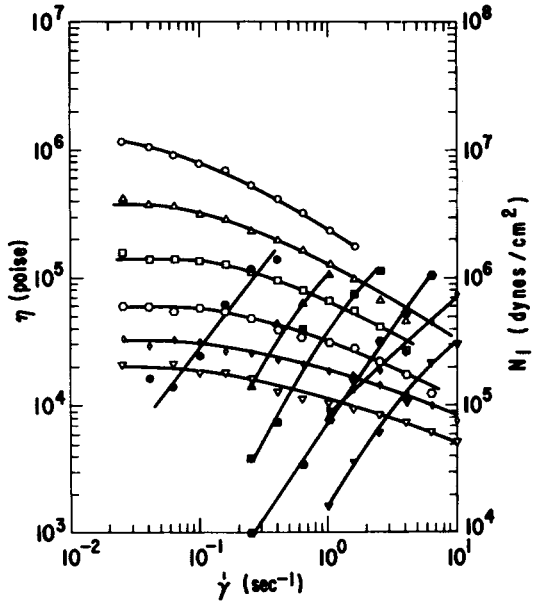

Fig. 8. Shear viscosity and primary normal stress difference as functions of shear rate for high-impact polystyrene: (○) η (●) N_1, 180°C; (△) η (▲) N_1, 200°C; (□) η (■) N_1, 220°C; (○) η (●) N_1, 240°C; (◇) η (◆) N_1, 260°C; (▽) η (▼) N_1, 280°C.

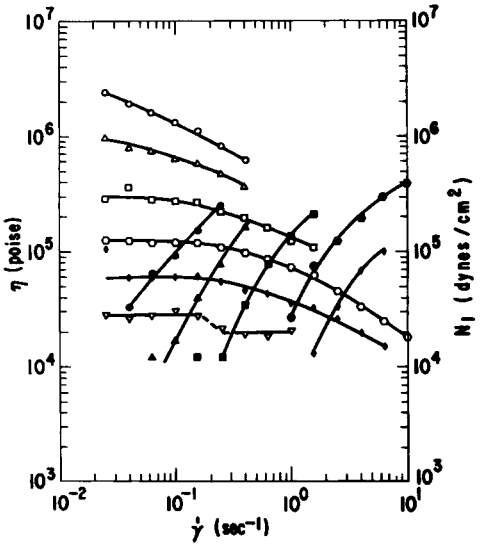

Fig. 9. Shear viscosity and primary normal stress difference as functions of shear rate for a 35–65 blend: (○) η (●) N_1, 200°C; (△) η (▲) N_1, 220°C; (□) η (■) N_1, 240°C; (○) η (●)N_1, 260°C; (◇) η (◆) N_1, 280°C; (▽) η (▼) N_1, 300°C.

the gap was set in about 15 min, but residual stresses from loading did not relax out. The data were collected despite this high residual stress (1.2×10^6 dynes/cm^2). This problem was even more serious at 260°C. Consequently, normal forces associated with the flow field could not be separated from the total normal force.

Since activation energy for flow is of interest with these materials, the steady shear viscosity of PPO resin was computed from the dynamic data using the Cox–Merz empirical relationship[6]

$$|\eta^*| = \left(\frac{G'^2 + G''^2}{\omega^2}\right)^{1/2} \tag{9}$$

where $\dot{\gamma}$ is set equal to ω. In earlier studies[7,8] the Cox–Merz relationship gave excellent agreement between $|\eta^*|$ and the steady shear viscosity of polypropylene. For the HIPS and the 35–65 blend, $|\eta^*|$ is in reasonably good agreement with the measured steady shear viscosity (Figs. 10 and 11). The differences in the two sets of PPO data (Fig. 7, 260° and 280°C) are most probably due to the high residual loading stress which remained throughout the test. As seen in Figures 7, 8, and 9, all three materials display a viscosity trend with a Newtonian flow region (independent of shear rate) and a shear sensitive region where the viscosity decreases with increasing shear rate.

Activation energy for flow is of interest with these polymers since it reflects the ease or difficulty with which molecules or molecular segments move in a flow field. The bulk movement of a molecule is a combination of many different relaxation processes which involves the translation of kinks or defects through an entire chain. Thus, polymer chains appear to flow by successive jumps of segments. The total energy for these processes provides insight into the size of the basic flow unit, hence viscosity, at a particular temperature and deformation rate. The Arrhenius equation is frequently used to relate viscosity to temperature, as follows[9]:

$$\eta = A \exp \frac{-E}{RT} \tag{10}$$

where A is a constant, E is the activation energy, R is the universal gas constant, and T is absolute temperature. Activation energies can be computed either at

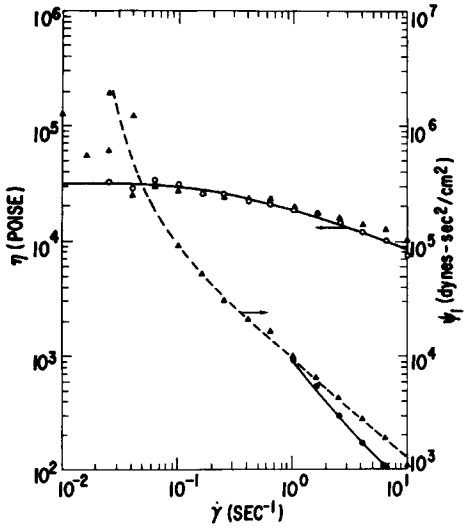

Fig. 10. Shear viscosity and primary normal stress coefficient as functions of shear rate for high-impact polystyrene; T = 260°C: (○) η (●) ψ_1, steady shear; (△) $|\eta^*|$; (▲) $\psi_1 = 2G'/\omega^2$.

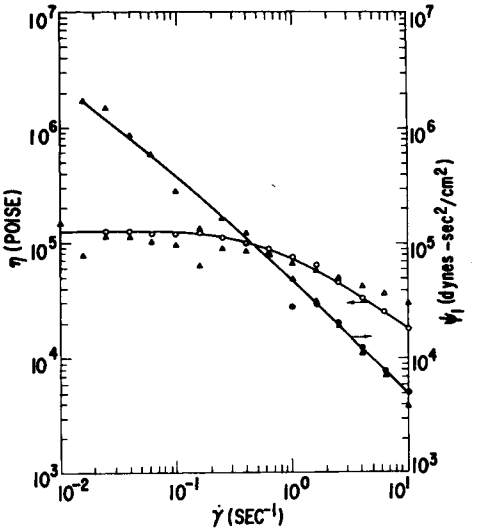

Fig. 11. Shear viscosity and primary normal stress coefficient as functions of shear rate for a 35–65 blend; T = 260°C: (○) η (●) ψ_1, steady shear; (△) $|\eta^*|$; (▲) $\psi_1 = 2G'/\omega^2$.

constant shear stress or at constant shear rate. The activation energies summarized in Table III are for the Newtonian region (zero shear rate) and for a shear rate of 1 sec^{-1}, which is within the shear-sensitive region. These energies were determined from a semilogarithmic plot of η versus $1/T$, which was linear over most of the temperature range. The activation energies indicate that the relaxation processes of PPO molecules are much more energetic than HIPS and that these processes are rather sensitive to the total deformation of the molecule since much less energy is required at the higher shear rate. The activation energy for the blend lies between the PPO resin and HIPS, again demonstrating rheological compatibility. A reasonable prediction of the activation energy for the blend can be computed from the following simple expression:

$$\frac{1}{E_B} = \frac{X_{PPO}}{E_{PPO}} + \frac{X_{HIPS}}{E_{HIPS}} \tag{11}$$

where X is the weight fraction of each component and B (blend), PPO, and HIPS refer to the three individual materials. A similar expression has been reported for estimating the glass transition temperature T_g of a blend when the glass transition temperatures for PPO resin and PS are substituted for activation energies.[2] The T_g of each material (compression-molded sheet) was measured by differential scanning calorimetry and found to be 203°C for PPO resin, 97°C for the polystyrene in HIPS, and 125°C for the 35–65 blend. The T_g form of eq. (11) predicts a T_g of 119°C for the 35–65 blend.

TABLE III
Flow Activation Energy E

Material	E, kcal/mole	
	$\dot{\gamma}$ = 0 sec^{-1}	$\dot{\gamma}$ = 1.0 sec^{-1}
HIPS	15.8	14.8
PPO Resin	46.9	34.2
35–65 Blend	23.6	18.2

With both HIPS and the 35–65 blend the loading stress relaxed out in a relatively short time so that torque and normal force could be measured as a function of shear rate. Normal force for PPO resin can be estimated with another empirical expression which was first proposed by Coleman and Markowitz[10] as a limiting relationship when the shear rate goes to zero. This relationship is expressed as the primary normal stress coefficient ψ_1 as follows:

$$\psi_1 = N_1/\dot{\gamma}^2 = 2G'/\omega^2 \tag{12}$$

with $\dot{\gamma} = \omega$. With HIPS at 260°C, eq. (12) shows considerable deviation from experimental values (Fig. 10). However, for the blend at 260°C, the agreement is excellent between experiment and eq. (12) (Fig. 11). In general, the agreement was between fair and good over the entire temperature range.

The viscosity and primary normal stress difference were also replotted on master curves (not shown). With viscosity, though, a vertical shift was required in addition to the horizontal shift in order to superpose all of the data onto one curve. The need for a vertical shift was anticipated since the molecular theory of viscoelasticity relates the shift factor to relaxation time τ, which is related to viscosity with the following expression[11]:

$$a_T = \tau_T/\tau_{T_0} = \eta\rho_0 T_0/\eta_0 \rho T \tag{13}$$

where ρ is density and the term $\rho_0 T_0/\rho T$ accounts for the thermal expansion between some temperature T and the reference temperature T_0. For many polymers this term is nearly equal to unity, which was the case for the three materials characterized in this study. This result was determined from the modulus data since

$$G''(\omega) = (\rho T/\rho_0 T_0)G''(\omega_0) \tag{14}$$

for

$$\omega = a_T\omega_0 \tag{15}$$

Since modulus data were superpositioned with only a shift in frequency, the term $\rho T/\rho_0 T_0$ must be essentially unity. Using this condition in eq. (13) yields

$$\eta(\dot{\gamma}) = a_T\eta(\dot{\gamma}_0) \tag{16}$$

for

$$\dot{\gamma} = a_T\dot{\gamma}_0 \tag{17}$$

When data are empirically shifted, Bird et al.[12] point out that the shift factors in eqs. (15), (16), and (17) are not expected to be equal but should not be widely different. The normal stress data, being like the modulus data, required only a horizontal shift to superposition the data. Hence, five different shift factors could be determined for each material and were for HIPS and the blend. Only four shift factors were computed for PPO resin because the normal force data could not be obtained. These shift factors are shown as a function of temperature in Figures 12 through 14 for a reference temperature of 260°C. Also shown in these figures is a curve computed from the WLF equation[11]

$$\log a_T = \frac{-C_1(T - T_0)}{C_2 + (T - T_0)} \tag{18}$$

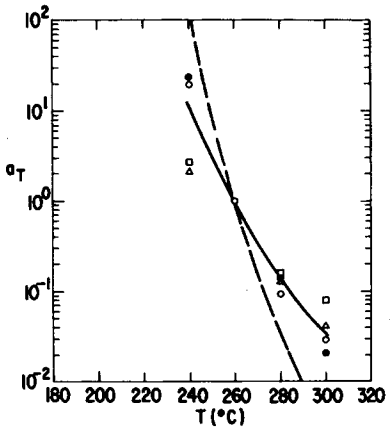

Fig. 12. Temperature dependence of empirical shift factors for poly(2,6-dimethyl-1,4-phenylene oxide) compared to WLF prediction with universal constants; $T_0 = 260°C$: (○) $\omega_{G'}$; (●) $\omega_{G''}$; (△) η; (□) $\dot{\gamma}_\eta$; (- -) WLF.

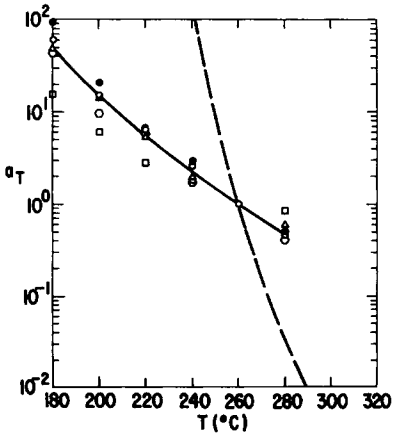

Fig. 13. Temperature dependence of empirical shift factors for high-impact polystyrene compared to WLF prediction with universal constants; $T_0 = 260°C$: (○) $\omega_{G'}$; (●) $\omega_{G''}$; (△) η; (○) $\dot{\gamma}_{N_1}$; (□) $\dot{\gamma}_\eta$; (- -) WLF.

where C_1 and C_2 are arbitrary constants but for comparison purposes were chosen as the universal constants $C_1 = 8.86$ and $C_2 = 101.6$. These values provided the best fit of experimental data for many different polymers.[11] All three materials in this investigation differ considerably from the WLF prediction using the universal constants. The smallest deviation occurs for PPO resin ($T_0 = T_g + 57°C$), which was expected since the above universal constants are recommended for a reference temperature which is less than 43°C above the polymer T_g. For HIPS ($T_0 = T_g + 163°C$) and the blend ($T_0 = T_g + 135°C$), large deviations from the WLF prediction are shown in Figures 13 and 14 (broken line). The form of the WLF equation, however, appears correct since the data in Figures 12, 13, and 14 can be curve fitted by the WLF equation with unspecified constants. Table IV summarizes the constants obtained by curve fitting the data for each material. These constants were computed from the average shift factors in Figures 12, 13, and 14, i.e., solid curves.

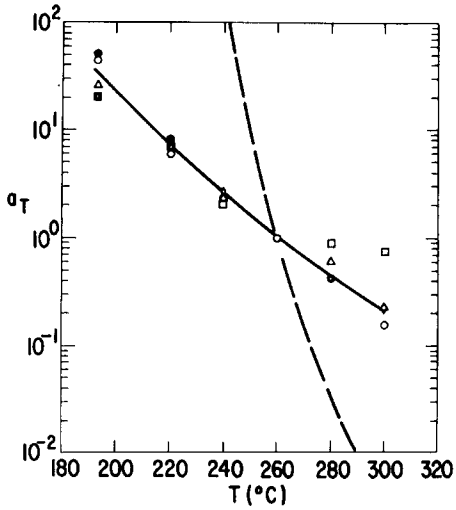

Fig. 14. Temperature dependence of empirical shift factors for a 35–65 blend compared to WLF prediction with universal constants; T_0 = 260°C: (○) $\omega_{G''}$; (●) $\omega_{G'}$; (△) η; (◇) $\dot{\gamma}_{N_1}$; (□) $\dot{\gamma}_\eta$; (- -) WLF.

TABLE IV
Empirical Constants for WLF Equation

Material	C_1	C_2
PPO Resin	9.59	154.3
HIPS	6.47	384.3
35–65 Blend	5.98	327.9

The shift factor, like the activation energy for flow, provides information on the molecular or segmental relaxation processes. While the activation energy (independent of temperature over a limited range) indicates the effect of deformation or deformation rate on molecular movement, the shift factor (independent of deformation rate) indicates the temperature dependence of the relaxation processes. Figures 12 and 13 clearly show that the temperature dependence of the relaxation processes in PPO molecules is very different from the temperature dependence of HIPS molecules. Despite these large differences, the blend displays relaxation processes, which depend on temperature, quite similarly to HIPS relaxations. The dispersed PPO molecules appear to have little effect on the temperature behavior of the HIPS relaxations. The activation energy for flow (Table II), on the other hand, shows that relaxation processes are strongly dependent on the molecular species.

The solid curves in Figures 12, 13, and 14 represent an average trend that could be used to shift any type of viscoelastic data if the data exist at only one temperature. Thus, considerable time can be saved when estimating viscoelastic material responses for different polymer processing operations.

The relaxation spectrum for each material was calculated using the loss modulus data shown in Figure 15. The approximate method of Ninomiya and Ferry[11] was used to calculate these spectra. This method involves a numerical differentiation, but requires no slopes in the computation. Instead, moduli values equally spaced above and below a specific point on the modulus curve are

weighted and summed to give the relaxation function at the point. The following formula was used:

$$H(\tau) = \frac{2}{\pi}\left\{G''(\omega) - \frac{b}{(b-1)^2}[G''(b\omega) + G''(\omega/b) - 2G''(\omega)]\right\} \quad (19)$$

where $\tau = 1/\omega$ and b is a constant which was set equal to 2.0.

The relaxation spectra for the three materials are shown in Figure 15. As expected from the low-frequency data, the PPO response extends to much longer relaxation times compared to HIPS. This is probably due to the translation of segmental motions along PPO chains involving more complex flow or relaxation mechanisms than those involved in HIPS chains. These mechanisms are also more energetic, as previously mentioned when activation energy for flow was discussed. The scatter in the computed data points at long relaxation times is the result of relatively large errors in the modulus data at the highest temperatures and lowest frequencies where both F_x and F_y are very small.

The relaxation plateau for PPO resin, corresponding to the rubbery region, is higher than the HIPS plateau which seems to be related primarily to the entanglement MW. Further support of this statement is some recent data that show that increasing PPO resin MW does not change the plateau value or short time response but adds relaxation processes with characteristically long times. The effect of PPO resin MW and MWD on the relaxation spectrum will be discussed in greater detail in a subsequent paper.[13] A similar trend in relaxation spectra has been reported by Onogi et al.[14] for fractionated PS samples.

When the effect of MW on the relaxation spectrum is known, the implication from Figure 15 is that the relaxation spectrum of a blend can be precisely tailored by physical mixing. Thus, an optimum balance between melt rheology and mechanical properties should be achievable. The long relaxation times of PPO resin which make melt processing difficult could be reduced to a level which improves melt processing without substantially compromising mechanical properties.

Mechanical properties of PPO–PS mixtures as a function of composition have been reported by Yee[16] who found at low temperatures (−190°C to −50°C) that

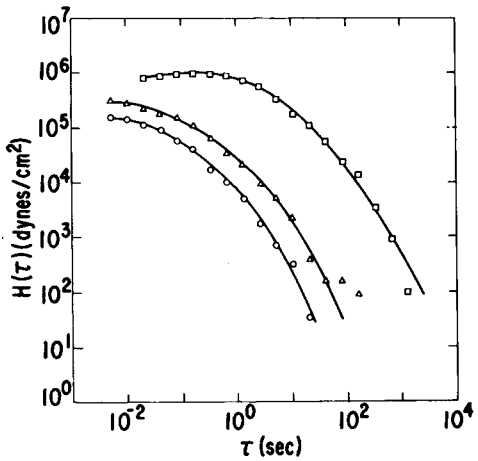

Fig. 15. Relaxation time spectra for poly(2,6-dimethyl-1,4-phenylene oxide), high-impact polystyrene, and 35–65 blend; T_0 = 260°C: (○) HIPS; (△) 35–65 blend; (□) PPO.

the secondary relaxations of the homopolymers were suppressed in the mixtures. However, at temperatures near and above 0°C, the secondary relaxations of homopolymers are increased by the presence of the other component. There was a maximum in tensile strength at each strain rate tested and all compositions failed at a higher stress level than either of the pure homopolymers. Additional studies are in progress to develop case histories which will explore the relationship of relaxation times to melt processing and mechanical properties.

Once again the response of the blend is an addition of PPO resin and HIPS relaxation processes, suggesting good mixing on a segmental level over the entire distribution of segments. This general rheological compatibility is rather remarkable considering that each polymer is highly entangled before physical mixing and the viscoelastic properties are vastly different. Despite these large differences, the PPO resin is very well dispersed in the HIPS. Apparently the high shear in the extruder and the favorable thermodynamics of this system drive the blend to a high intensity of mixing. Even the entanglement MW, indicated by the rubbery plateau, falls between the two pure components.

For all of the rheological data obtained on the blend, there were no distinguishable effects produced by the small amount of stabilizers.

CONCLUSIONS

The viscous and elastic responses of pure HIPS and pure PPO melts have been shown to be widely different. On a molecular level or segmental level, relaxation processes in PPO resin are two to three times more energetic than relaxations in HIPS. The temperature dependence of the relaxation times are also very different for these materials. The shift factors for each material follow a WLF equation, but with a different set of constants for each material. Despite these large differences in viscoelastic behavior, a 35–65 blend exhibited general rheological compatibility with material parameters and responses being intermediate between the two pure components. The computed relaxation spectra for the three materials indicate good segmental mixing in the blend over the entire distribution of chains and chain segments.

The resins were compression molded into sheets by E. M. Lovgren. S. R. Weissman ran the intrinsic viscosities, P. E. Gundlach obtained the GPC results, and A. L. Young measured the T_g of each material. The many stimulating discussions with G. F. Lee, Jr., throughout the various phases of this work are greatly appreciated. The author is also indebted to Drs. A. R. Shultz and C. J. Aloisio (Bell Laboratories) for many useful comments and suggestions.

References

1. J. A. Manson and L. H. Sperling, *Polymer Blends and Composites,* Plenum, New York, 1976.
2. A. R. Shultz and B. M. Gendron, *J. Appl. Polym. Sci.,* **16,** 461 (1972).
3. A. R. Shultz and R. S. Porter, *J. Polym. Sci. A-2,* **10,** 1639 (1972).
4. K. Walters, *Rheometry,* Wiley, New York, 1975.
5. R. S. Marvin, in *Viscoelasticity,* J. T. Bergen, Ed., Academic, New York, 1960.
6. W. P. Cox and E. H. Merz, *J. Polym. Sci.,* **28,** 118 (1958).
7. D. L. Faulkner and L. R. Schmidt, *Polym. Eng. Sci.,* **17,** 657 (1977).
8. D. L. Faulkner and L. R. Schmidt, *Technical Proceedings, 32nd Annual Technical Conference, SPI,* Washington, D.C., Feb. 7–10, 1977.
9. J. M. McKelvey, *Polymer Processing,* Wiley, New York, 1962.
10. B. D. Coleman and H. Markovitz, *J. Appl. Phys.,* **35,** 1 (1964).

11. J. D. Ferry, *Viscoelastic Properties of Polymers,* Wiley, New York, 1970.
12. R. B. Bird, R. C. Armstrong and O. Hassager, *Dynamics of Polymeric Liquids, Vol. I, Fluid Mechanics,* Wiley, New York, 1977.
13. L. R. Schmidt, to be published.
14. S. Onogi, H. Kato, S. Ueki, and T. Ibaragi, *J. Polym. Sci. C,* **No. 15,** 481 (1966).
15. A. F. Yee, *Polym. Eng. Sci.,* **17,** 213 (1977).

Received June 15, 1978